

Rutgers Lecture
May 10, 2009
F.H. Stillinger
View 1

MODELING PREBIOTIC APPEARANCE OF BIOLOGICAL CHIRALITY

Thomas G. Lombardo, Pablo G. Debenedetti
Chemical Engineering Dept., Princeton

Frank H. Stillinger
Chemistry Dept., Princeton

Published version to appear in PNAS Feature Issue entitled:
"Liquids and Structural Glass Formers"
(David Chandler, organizing editor)

Financial Support: NSF Collaborative Research in Chemistry Grant

MODELING PRE-BIOTIC APPEARANCE OF BIOLOGICAL CHIRALITY
[101st Statistical Mechanics Conference, Rutgers Univ., May 10, 2009]

View 1. Title, collaborators, PNAS issue, NSF support

One of the more intriguing challenges presented by molecular biology is why so many of the chemical building blocks out of which living organisms are formed display an almost completely broken symmetry with respect to right and left hand geometries. In other words terrestrial life exhibits a single chirality. As emphasized in View 2 this is evident in observed molecular structures of proteins, DNA, carbohydrates, and other biopolymers.

MOTIVATING MYSTERIES

- Biological molecules (proteins, DNA, carbohydrates,) occur overwhelmingly with chiral subunits that exhibit only one of the two possible mirror image forms.
- How did this broken geometric symmetry arise?
- Is the spontaneous appearance of life and its subsequent evolution possible only in such a symmetry-broken chemical environment?
- How far must one search in the universe to find C,N,O,H based life with the opposite chirality?

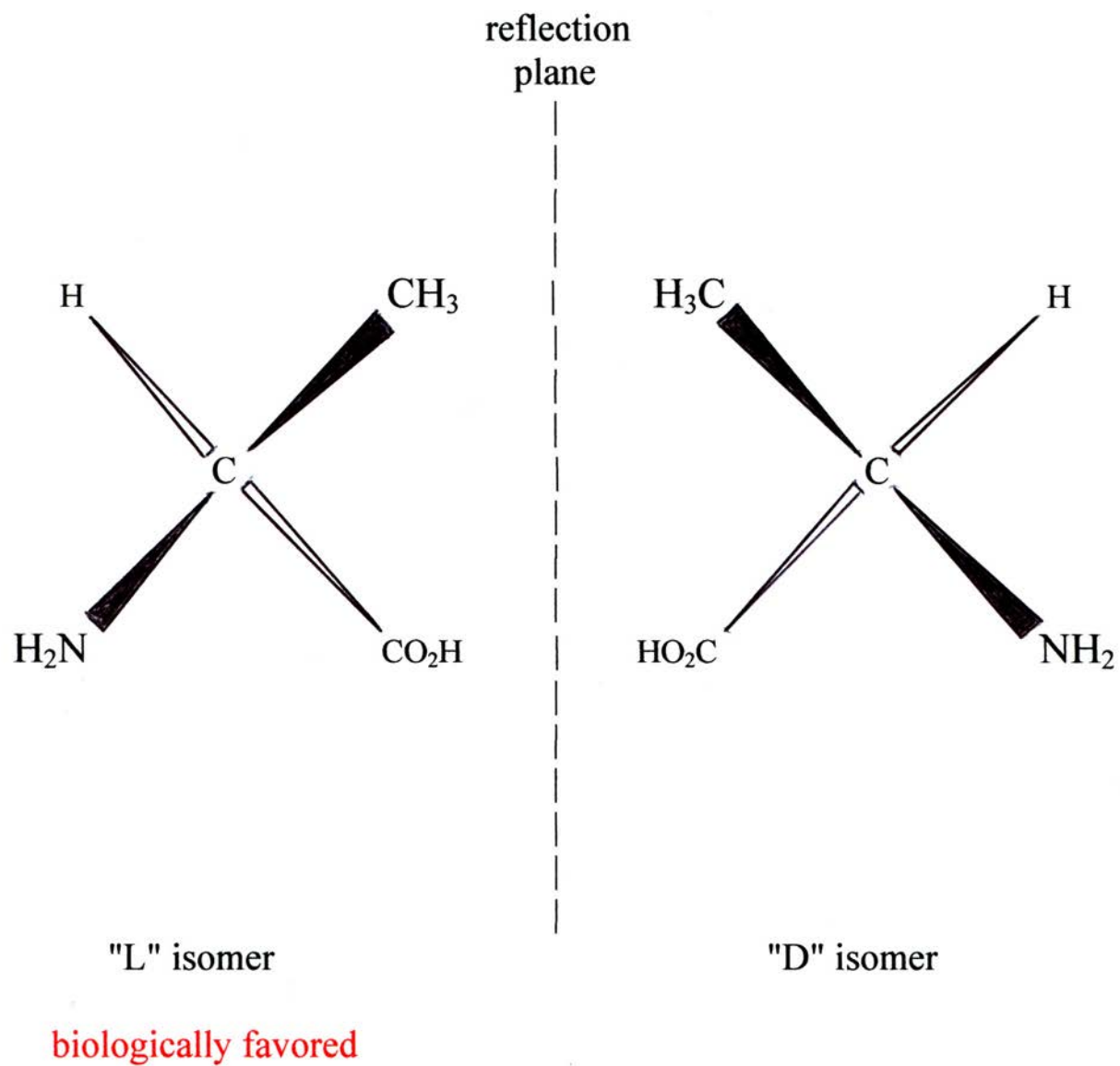
View 2. Motivating mysteries

These observations naturally raise basic questions: (a) how did this broken geometric symmetry arise on the early earth, and (b) is the appearance of life and its subsequent evolution contingent on such broken symmetry? It also leads astrobiologists to wonder about the presence of opposite chirality elsewhere in the universe.

It may never be possible to attain definitive answers to these questions. However it is feasible to explore possible physical and chemical scenarios that conceivably could have produced the observed broken symmetry. In that spirit the purpose of this short lecture is to propose and describe one model for a possible contributor to the present terrestrial situation.

With one exception (glycine) the amino acids serving as the building blocks of proteins individually are chiral. They exhibit only one form in terrestrial biology. The following View 3 illustrates this for the specific case of alanine.

AMINO ACID EXAMPLE: ALANINE



View 3. D and L forms of alanine.

The rigid tetrahedral bonding at the central carbon atom produces two distinct arrangements of the four attached groups. Biologically occurring alanine, either by itself or as a subunit in proteins, exhibits the so-called "L" form indicated on the left.

Not surprisingly this area has a long history of experiment and speculative theory. And not surprisingly it has spawned its own lexicon of chemical jargon. A few of its frequently used symbols, words, and phrases are displayed on View 4.

SOME CHEMICAL JARGON

Chirality: non-superposable with mirror image

Enantiomer: one (or the other) chiral form

D, L: identifying labels for the two enantiomers

R, S: another convention for labeling enantiomers

+, -: yet another labeling convention for enantiomers

Racemic: presence of equal amounts of the two enantiomers

Enantiomeric Excess: unequal concentrations of enantiomers,

$$\text{"EE"} = \frac{|x_D - x_L|}{x_D + x_L} \times 100\%$$

Asymmetric Amplification: increase in enantiomeric excess

Autocatalysis: enhanced synthesis rate of one enantiomer due to the prior presence of its own kind

View 4. Some chemical jargon

One confusing situation concerns the naming of the enantiomers -- the mirror image molecular twins. Each of the three alternatives has a precise definition, but they use basically different rules. In the case of amino acids whether free or incorporated in proteins the "D,L" convention is the usual choice.

The refereed published literature advocates several possible mechanisms for emergence of a dominating chirality. The next View 5 lists five of these.

POSSIBLE MECHANISMS

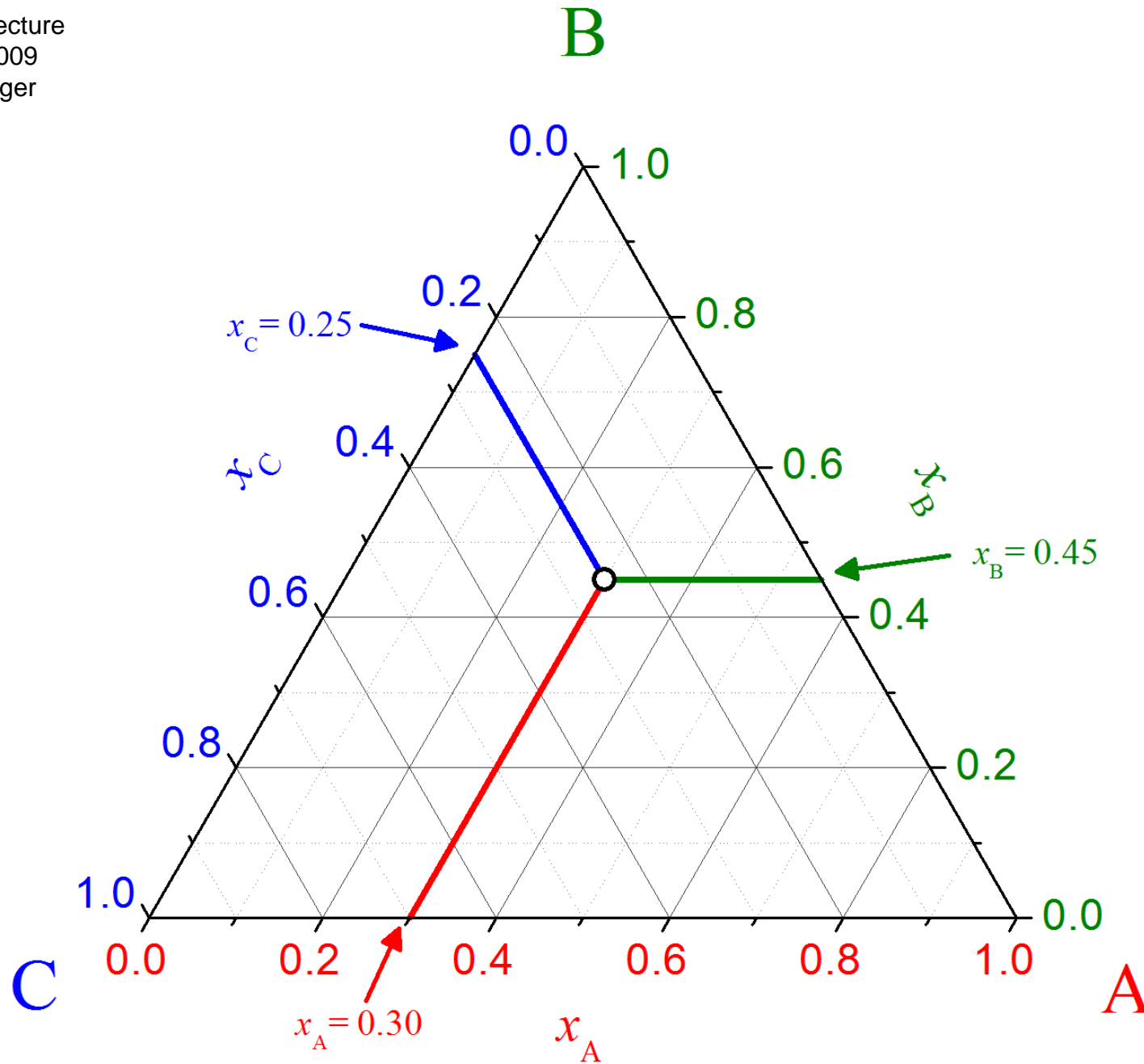
- (1) Parity-violating weak interactions
- (2) Illumination with circularly polarized light
- (3) D, L phase diagram characteristics
- (4) Liquid-phase chemical kinetics with autocatalysis
- (5) Mechanically disturbed crystallization with slow liquid-phase D, L interconversion, and "Ostwald ripening"

View 5. Possible mechanisms

The first entry involving weak interactions has been proposed but is almost certainly orders of magnitude too weak to be a serious contender. My Princeton colleagues and I have generated simple models illustrating scenarios (3) and (4). Limited time here will only allow presenting aspects of (3).

In fact our interest in (3) was stimulated by published experiments concerning relevant characteristics of equilibrium phase diagrams for three-component systems. In particular these experiments involved D and L forms of amino acids plus a relatively poor solvent.

Rutgers Lecture
May 10, 2009
F.H. Stillinger
View 6



View 6. Equilateral triangle for 3-component systems; fixed T,p

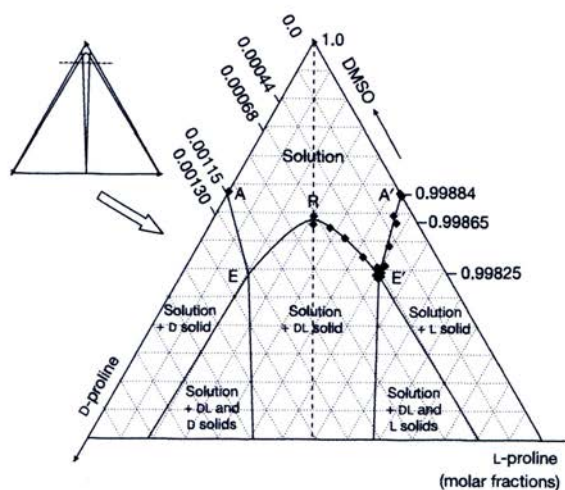
For those who might not be familiar with the conventional way that chemists and engineers graphically present those 3-component results View 6 shows the underlying convention based on an equilateral triangle whose vertices represent the pure species. The normal distances to opposite sides from those vertices are proportional to the respective mole fractions.

With that background on phase diagram display convention, the following View 7 presents a key experimental result from Imperial College, London published in Nature in 2006.

EXAMPLE FROM EXPERIMENT

M. Klussman, *et al.*, Nature **441**, 621-623 (2006), "Thermodynamic control of asymmetric amplification in amino acid catalysis"

Ternary phase diagram for D+L proline with achiral solvent "DMSO":



Evaporating solvent from racemic mixture encounters symmetry-breaking instability point \Rightarrow random initial enantiomeric excess in liquid phase becomes amplified.

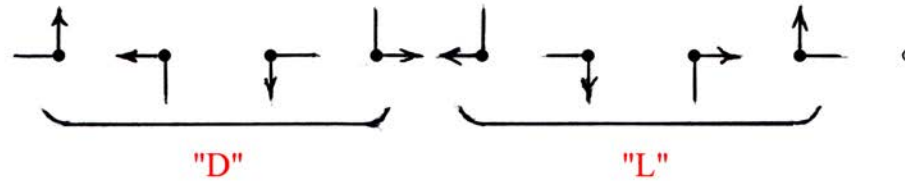
View 7. Phase diagram portion, D,L proline + DMSO; ambient conditions [Fig. 2, *Nature* article]

Because the non-chiral solvent DMSO is a rather poor solvent for the proline enantiomers, only a relevant small portion of the entire 3-component triangle near the pure-DMSO vertex is shown. Four distinct phase (as well as their coexistence regions) are shown: dilute liquid solution, pure D-proline and pure L-proline crystals, and a racemic D,L-proline crystal. Of course the diagram has bilateral symmetry about the vertical line passing through the DMSO vertex.

The significance of the experimental result is the appearance of the phase boundary maximum ("R") below the solution region, flanked by a pair of off-symmetry eutectic points. This produces a scenario roughly analogous to the familiar case of a zero-field ferromagnetic Ising model cooled reversibly from high temperature through its Curie point, with random small fluctuations steering it either to a fully up or fully down final spin state. The amino acid solution version starts with a virtually racemic very dilute solution very near the upper vertex, followed by solvent evaporation moving the state point downward toward the boundary maximum, then departing left or right to one of the eutectics. Which way it departs depends simply on which random small fluctuation in chiral molecule numbers happened accidentally to be present. Upon reaching the eutectic, the remaining liquid displays a macroscopic EE. The mechanism involves tying up equal numbers of D and L molecules in the racemic crystal. But keep in mind that the boundary maximum is not a solution critical point.

ELEMENTARY MODEL

- $2n \times 2n$ square lattice, periodic boundary conditions
- Site single occupancy with 9 states:



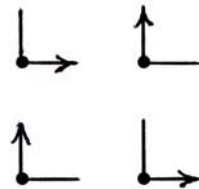
- Three interactions:
 - (1) $v_0 < 0$ for n.n. contact between any pairs of **D** and/or **L**, *e.g.*:



- (2) $v_1 < 0$ for identical **D** or **L** twins (same orientation), *e.g.*:



- (3) $v_2 < 0$, a 4-site interaction for **D** and **L** molecules alternating around a square, with identical bent backbone orientations, *e.g.*:



- System potential energy: $\Phi = v_0 N_0 + v_1 N_1 + v_2 N_2$

View 8. Elementary model, square lattice, 9 site states

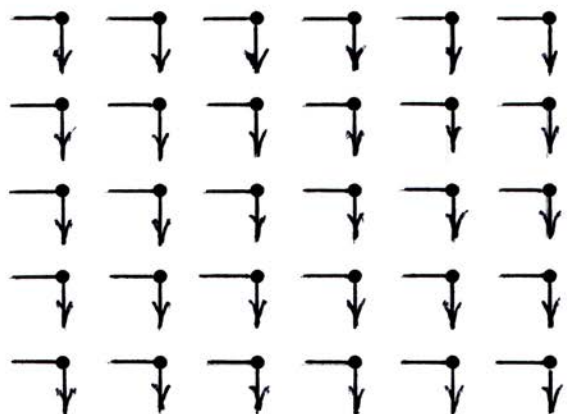
View 8 indicates how this kind of phase diagram might be approached theoretically using a "minimalist" classical model. It resides on the square lattice in two dimensions.

Each site of the lattice can host any one of nine states. Eight of these, shown as bent arrows, represent chiral molecules. The ninth state represents a non-chiral solvent. As shown, the "D" and "L" molecules each have four possible orientations, with their "arms" pointing to nearest-neighbor sites. Solvents are structureless. The enantiomorphs are not interconvertible, they are stable so initial composition remains unchanged.

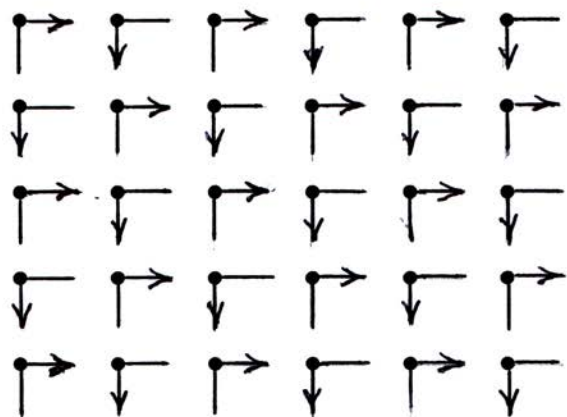
Three short-range interactions are postulated, each negative. The first (v_0) acts between any nearest-neighbor pair of chiral molecules regardless of their orientation or chirality; this controls the limited solubility required. The second (v_1) is an additional interaction for any nearest neighbor pair of molecules that are identical twins with respect to both chiral character and orientation; this allows for stable pure-enantiomorph crystals when only solvent and one dominating enantiomorph are present. Finally a four-site interaction (v_2) arises for any elementary square of sites around which molecules reside with alternating chirality and common orientation of the bent backbones; this allows for existence of a stable racemic crystal.

FORMATION OF CRYSTALS AT LOW T

- Solvent plus pure D or L (8 possibilities):



- Solvent plus racemic D, L mixture (4 possible orientations):



Stability requires $v_2 < 2v_1 < 0$.

View 9. Formation of crystals at low T (or high concentration); interaction inequality

View 9 illustrates the pure-enantiomer and racemic crystal forms. Note that an inequality involving v_1 and v_2 must be obeyed to ensure stability of the latter.

Unfortunately no analytical method is available for exactly solving this nine-state two-dimensional model. We have relied on the well-known but obviously approximate mean-field approach, as outlined on View 10.

FREE ENERGY AND PHASE DIAGRAM ESTIMATION

- Apply the mean field approximation for the lattice's set of 9 site-occupancy states.
- Calculations done at fixed D, L, solvent composition.
- 2 sublattices require finding **6 order parameters** at each temperature and composition.
- Phase diagram determined by free energy minimization supplemented by Maxwell construction.
- Vary v_1/v_0 , v_2/v_0 and repeat calculation.

View 10. Free energy and phase diagram estimation

Mean-field approximations are unreliable when critical points are involved, but that is not the case here. We believe that approximation preserves the qualitative nature of the phase diagram for the model. The calculations are done at fixed composition (and T), and require free energy minimization with respect to 6 order parameters. The Maxwell construction has to be invoked to locate phase boundaries.

TYPICAL INTERACTION CHOICE FOR LIMITED ENANTIOMER SOLUBILITY AND STABLE RACEMIC CRYSTAL

$$v_0 = -1 ,$$

$$v_1 = -2 ,$$

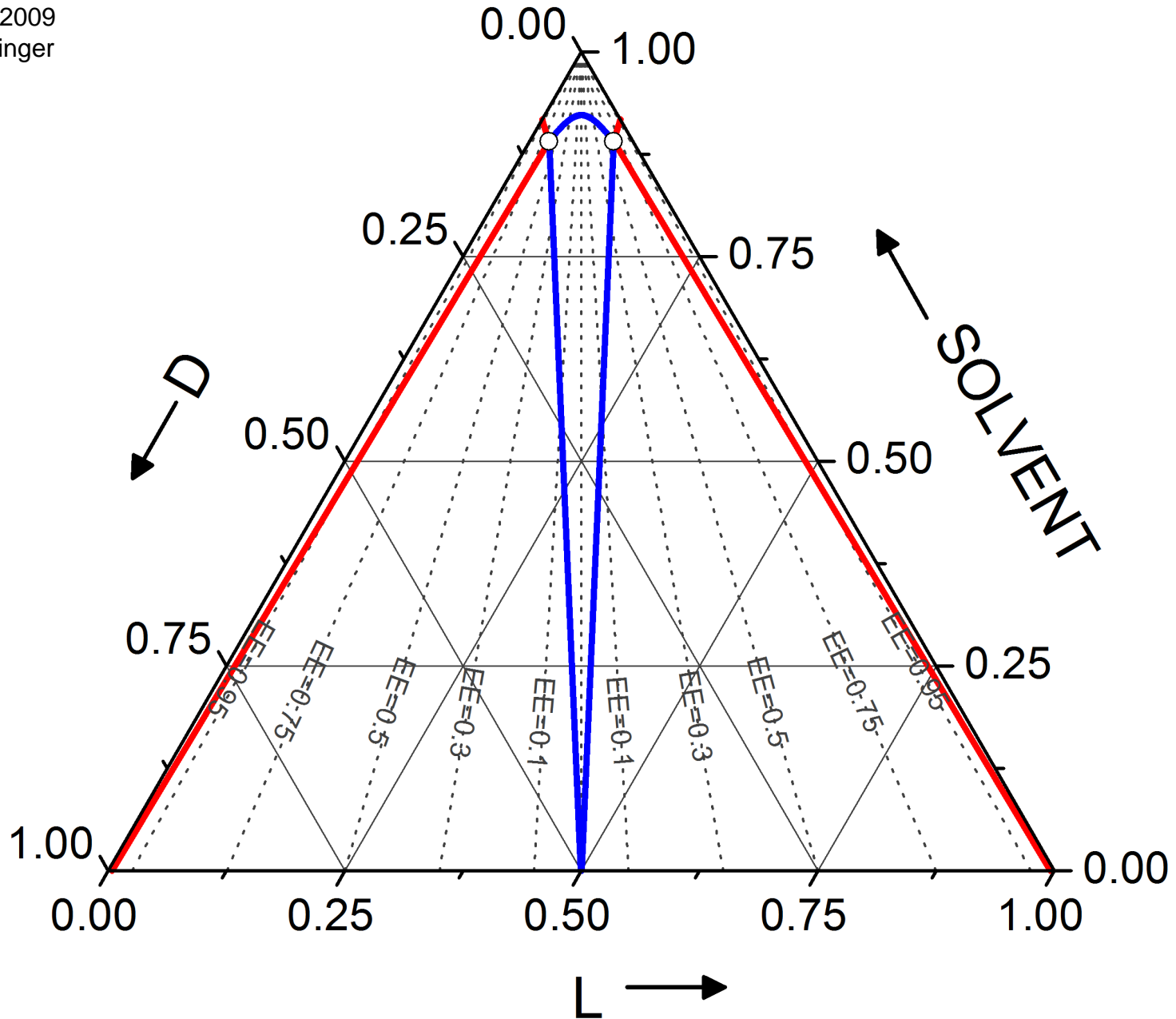
$$v_2 = -5 .$$

View 11. Typical interaction choice

View 11 presents a typical choice for the three negative interactions. This set satisfies the requirements set by the motivating experiments concerning limited solubility and existence and stability of enantiomeric and racemic crystal phases.

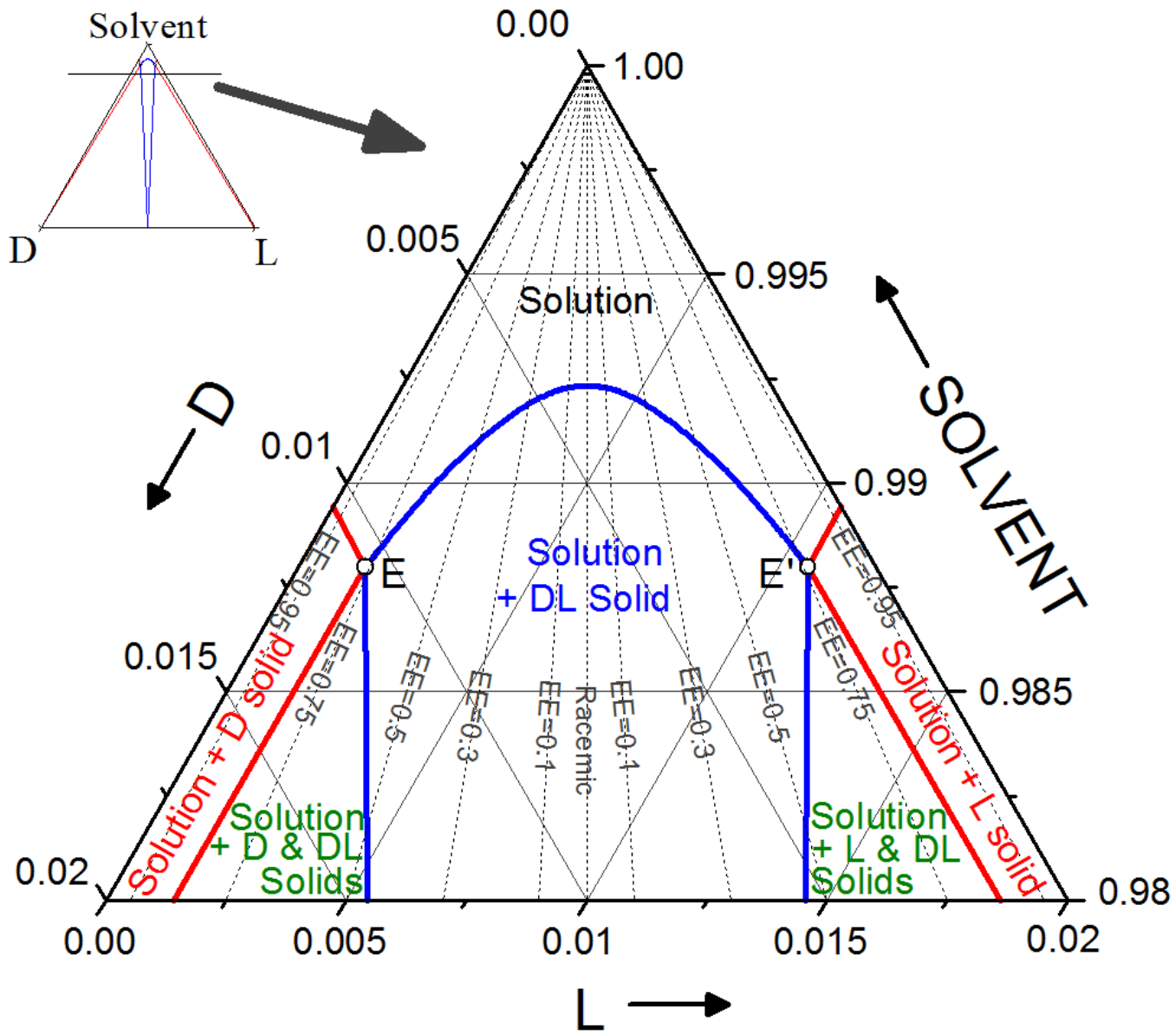
The computed phase diagram for that set of interactions (at $T=1$) appears in View 12.

Rutgers Lecture
May 10, 2009
F.H. Stillinger
View 12



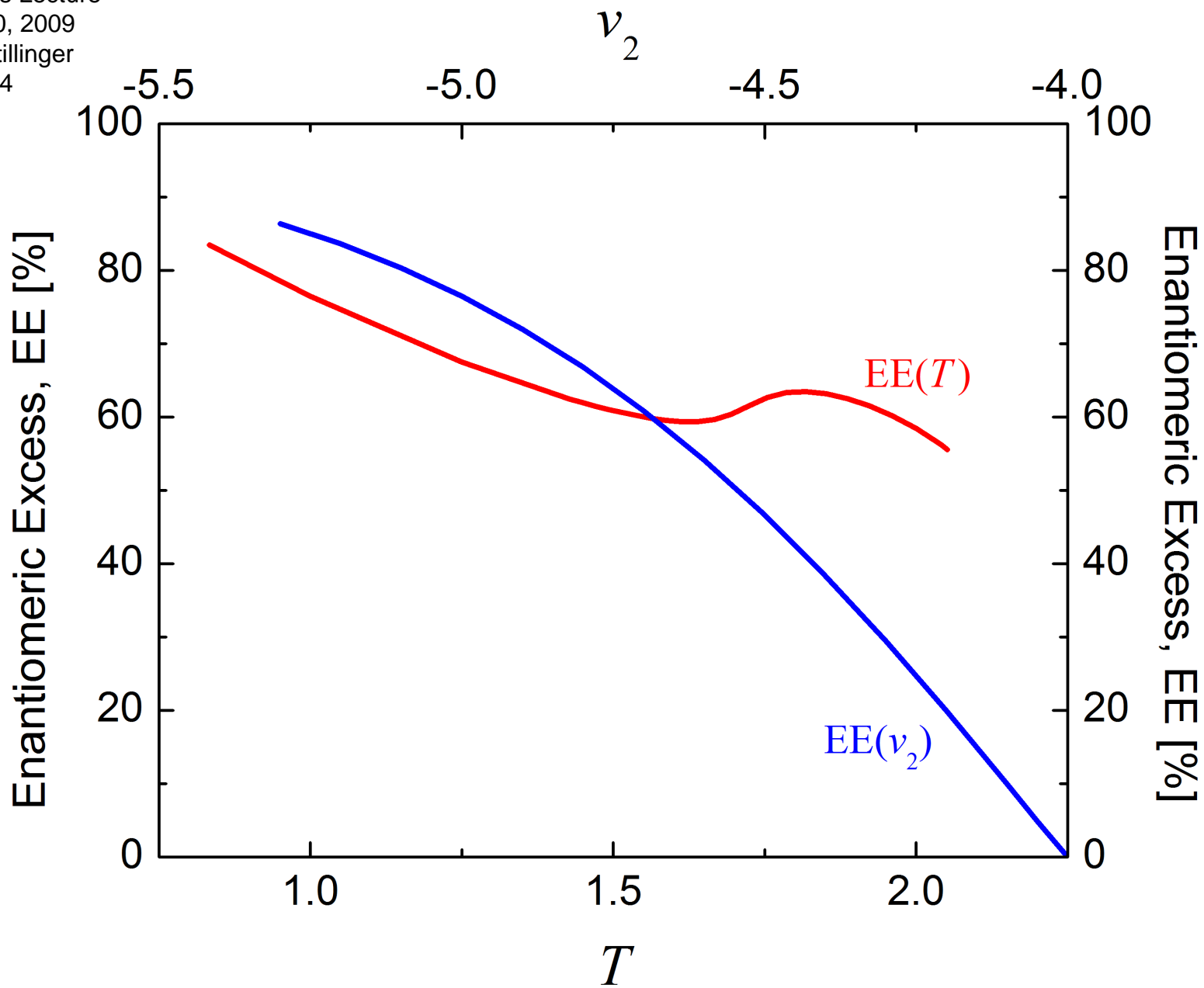
View 12. Full-triangle phase diagram for $v_0, v_1, v_2 = -1, -2, -5$
and $T=1$ [ternary(T=1)_full.png]

Thin red-outlined regions to left and right represent 2-phase coexistence of solution + enantiomorphous crystal, the blue-outlined region near the center is 2-phase coexistence of solution and racemic crystal. As required qualitatively, the portion of the diagram relevant to the motivating experiment is concentrated near the top. An expanded view of that top portion appears in the following View 13. Notice that the EE at each of the off-symmetry eutectic pair is approximately 75%.



View 13. Expanded view of the top portion of View 11
[model_ternary_T=1.png]

The same kind of mean-field calculations have been performed at different temperatures and with different interaction magnitudes. The phase diagrams remain similar for modest changes. But what is most significant is how the EE changes under these modifications.



View 14. EE variations with respect to T ($-1,-2,-5$ set),
and v_2 ($v_0, v_1 = -1, -2$) [EE(v2,T).png]

View 14 summarizes the kinds of changes that arise, where the red curve shows T variation for the $-1,-2,-5$ interaction set, while the blue curve indicates how EE changes as v_2 deviates from the original set, v_0 and v_1 remaining unchanged.

FINAL REMARKS

- Verification:** Monte Carlo simulation desirable to check accuracy of mean field approximation
- Generalization:** Easily extended to 3 dimensions and/or continuum versions
- Extension:** Minimalist models can also be developed for other credible symmetry-breaking processes
- Justification:** More prebiotic geochemistry and geophysics needed to assign likelihoods to the distinct symmetry-breaking scenarios

View 15. Final remarks

An appropriate conclusion consists of four brief remarks, View 15. These indicate the desirability of (1) confirming mean-field predictions by Monte Carlo simulation; (2) generalizing the model to 3 dimensions and/or a continuum (non-lattice) version; (3) extending minimalist modeling to other (non-equilibrium) scenarios for EE amplification; and (4) relying on experimental observations in prebiotic geochemistry and geophysics to assign likelihoods to the various scenarios that have been modeled.